RSC Advances

PAPER

View Article Online
View Journal | View Issue

Cite this: *RSC Adv.*, 2020, **10**, 1447

Influence of ceramic particles as additive on the mechanical response and reactive properties of Al/PTFE reactive composites

Jiaxiang Wu, Junyi Huang, Qiang Liu, Yong Chen, Yuchun Li,* Li Yang, Qin Yin, Zhenru Gao, Shuangzhang Wu and Xinxin Ren

Received 8th November 2019
Accepted 6th December 2019

DOI: 10.1039/c9ra09291a

rsc.li/rsc-advances

To investigate the influence of SiC and Al_2O_3 as additives on the mechanical response and reactive properties of Al/PTFE (aluminum/polytetrafluoroethylene) reactive composites, Al/SiC/PTFE and Al/Al_2O_3/PTFE samples with different component ratios were prepared for quasi-static compression and drop-weight tests. Al/Al_2O_3/PTFE samples with different particle sizes were prepared for simultaneous thermal analysis experiments. The stress–strain data, characteristic drop height and thermogravimetry-differential scanning calorimetry (TG-DSC) curves of the composites were recorded. The results show that the addition of SiC and Al_2O_3 significantly enhance the strength of Al/PTFE. The enhancing effect of SiC on the composite strength was stronger than that of Al_2O_3. The addition of SiC and Al_2O_3 contribute toward reducing the sensitivity of the composites, where the reducing effect of Al_2O_3 on Al/PTFE sensitivity was weaker than that of SiC. Nanoscale Al_2O_3 reacts with PTFE to form AlF_3, and the reaction heat decreases dramatically with an increase in the Al_2O_3 particle size. The addition of nanoscale Al_2O_3 improves the reaction heat and energy density of the composites.

1 Introduction

Reactive materials are newly developed energetic composites. They are generally composed of two or more solid materials that do not possess explosive properties. Reactive materials remain inert at room temperature and atmospheric pressure, and can undergo obvious chemical reactions under severe impact load.[1–3] These materials can consist of multi-functional structural materials including thermites, metal-fluoride polymer, metal-hydride mixtures and matrix materials.[4–6] They are usually prepared *via* a molding sintering method and have the characteristics of higher energy density, faster energy release rate and increased safety compared to traditional explosives such as trinitrotoluene (TNT) and cyclotrimethylenetrinitramine (RDX).[7] It is well known that fluorine has the highest electronegativity of all the elements. Strongly oxidizing fluorine-containing free radicals are released when fluoropolymers are decomposed upon heating, with PTFE having the highest fluorine content of all fluoropolymers.[8] Therefore, it is suitable for use as an oxidant in reactive materials. Based on this, among all the different types of reactive materials, Al/PTFE (aluminum/polytetrafluoroethylene) has attracted widespread attention and has been extensively studied.[9–11]

Al/PTFE is both a composite and energetic material, thus, the experimental research should not only focus on the study of its mechanical properties, but attention needs to be paid to the reaction characteristics of the materials. For the purpose of the successful application of Al/PTFE, it is necessary to ensure that Al/PTFE has enough strength to guarantee its safety during production, storage and explosive loading, meanwhile, it can also generate exothermic reactions while penetrating the target. Wang *et al.* [12] investigated the penetration enhancement behavior of an Al/PTFE double-layered linear shaped charge against thick steel targets. The experimental results and numerical simulations indicate that its penetration performance and reactive material mass entering the penetrated target strongly depended on the reactive liner thickness and standoff. And, the initiation delay time of Al/PTFE rose evidently with an increase in the reactive liner thickness. Feng *et al.*[13,14] observed an intense reaction phenomenon of a Al/PTFE sample treated by a specific sintering process under quasi-static compression for the first time. Based on this discovery, the impact exerted by sintering temperature, component ratio and Al particle size on the quasi-static reaction of Al/PTFE were investigated. Wang *et al.*[15] studied the effect of temperature on the mechanical properties and reactive behavior of Al/PTFE under quasi-static compression. Scanning electron microscopy results showed that the temperature played a very momentous role in the fracture mechanisms of PTFE. The material went through brittle–ductile transformation related to a temperature-induced phase transition of the PTFE matrix.

In recent years, extensive research has been conducted on the application of additives in reactive materials to tune the

College of Field Engineering, Army Engineering University of PLA, Nanjing, 210007, China. E-mail: liyuchunmail@163.com

reactivity of composites.[16,17] He *et al.*[18] utilized a synthesized polydopamine binding layer to adjust the reactivity of nanoscale Al/PTFE, where it was found that the mixture of PTFE and nanoscale Al coated with polydopamine showed increased energy release and reduced sensitivity, and more importantly tunable reactivity. In order to improve the strength and density of materials, metal particles are also very common additives, such as W particles. Wang *et al.*[19] investigated the mechanical behavior and impact insensitivity of Al/W/PTFE composites with different W percentage, and the results indicate that the strength under dynamic compression loading and insensitivity under impact loading of Al/W/PTFE composites show an increasing tendency with increased W content. Cai *et al.*[20] and Herbold *et al.*[21] carried out research on the influence of particle size on the mechanical properties, failure and shock behavior of Al/W/PTFE. The numerical results reveal that the strength of Al/W/PTFE decreased as the W particle size rose owing to the function of force chains. However, W cannot participate in the reaction and only acts as a mass carrier in the materials system, which leads to a decrease in the energy density of the materials.

Previous studies show little research on the properties of Al/PTFE after adding ceramic materials. As typical ceramic particles, SiC and Al_2O_3 possess the excellent characteristics of high hardness and outstanding wear resistance. Osborne *et al.*[22,23] reported a pre-ignition reaction (PIR) phenomenon that was controlled by the fluorination of the Al particle passivation shell (Al_2O_3) when nano-Al/PTFE was heated over 400 °C. Consequently, it can be considered that SiC and Al_2O_3 can be used as additives to increase the energy density while improving the mechanical properties of the composites. Because the raw material ratio and particle size have great effects on the properties of materials, Al/SiC/PTFE and Al/Al_2O_3/PTFE samples with different component ratios were prepared for quasi-static compression and drop-weight tests. Considering that SiC cannot react with Al/PTFE, the thermal behavior of Al/SiC/PTFE was not investigated, only Al/Al_2O_3/PTFE samples with different particle sizes were prepared for simultaneous thermal analysis experiments. The influence of SiC and Al_2O_3 as additives on the mechanical response and reactive properties of Al/PTFE reactive composites were ascertained.

2 Experimental

2.1 Materials

The initial powders used to prepare the samples have the following average size: PTFE: 25 μm (from 3 M, Shanghai, China); SiC: 7 μm (from Yinuo, Qinhuangdao, China); Al_2O_3: 30 nm, 1 μm (from Naiou, Shanghai, China); Al: 50 nm, 1 μm (from Naiou, Shanghai, China).

2.2 Sample preparation

For the quasi-static compression and drop-weight tests, four types of Al/SiC/PTFE and Al/Al_2O_3/PTFE samples with different mass ratios were prepared. The particle sizes of Al and Al_2O_3 were 1 μm. The mass fractions of the ceramic particles were 0, 10%, 20%, 30% and 40% respectively. The ratio of Al to PTFE in the remaining mass fraction was based on the chemical equilibrium ratio (26%/74%). Table 1 tabulates the formulations of the experimental samples, along with the corresponding theoretical maximum density (TMD). The preparation process was based on Nielson's patent, which includes mixing, cold isostatic pressing and vacuum sintering.[24] The raw materials were stirred mechanically for 20 min in an ethanol solution and dried for 48 h at 60 °C in a vacuum oven. Then, the dried powder was cold pressed using an FLS30T hydraulic press under a compressive pressure of 300 MPa to obtain cylindrical samples with sizes of Φ10 mm × 10 mm (for the quasi-static compression tests) and Φ10 mm × 3 mm (for the drop-weight tests). Finally, the pressed samples were sintered in a vacuum oven at 360 °C for 6 h at a heating rate of 90 °C h^{-1} and a cooling rate of 50 °C h^{-1}.

For thermogravimetry-differential scanning calorimetry (TG-DSC) tests, Al (50 nm)/Al_2O_3 (30 nm)/PTFE, Al (1 μm)/Al_2O_3 (30 nm)/PTFE and Al (1 μm)/Al_2O_3 (1 μm)/PTFE were mixed according to the mass ratios 22/63/15%. To better understand the thermal reaction process of the composites, Al (50 nm)/PTFE, Al (1 μm)/PTFE, Al_2O_3 (30 nm)/PTFE and Al_2O_3 (1 μm)/PTFE were prepared as references with a mass ratio of 26/74%. All mixtures were sonicated in ethanol solution for 20 min *via* an ultrasonic mixing method to make even dispersed powders, then the mixtures were dried in a vacuum oven for 24 h at 60 °C.

For the purpose of examining the homogeneity of the prepared composites, sections of the samples before sintering were photographed using a Hitachi S-3400N II scanning electron microscope (SEM) to investigate the interior microstructures of the composites (Fig. 1). The geometry of the Al particles is spherical, while those of the SiC and Al_2O_3 are irregular. It can be found that Al, SiC and Al_2O_3 are uniformly distributed in the PTFE matrix, indicating that the initial powders were homogeneously mixed through the preparation process outlined. Arising from the applied tensile force when specimens were broken off, PTFE fibers could be easily observed in the microstructures of the specimens.

2.3 Experimental procedures

Quasi-static compression tests were carried out using a CMT5105 electrohydraulic press (MTS industry system Co.

Table 1 Formulations and TMDs of experimental samples for quasi-static compression and drop-weight tests

Type	Al/wt%	PTFE/wt%	Ceramic particles/wt%	TMD/g cm^{-3}
A	26.0	74.0	0	2.31
B	23.4	66.6	10 (SiC)	2.38
C	20.8	59.2	20 (SiC)	2.45
D	18.2	51.8	30 (SiC)	2.52
E	15.6	44.4	40 (SiC)	2.59
F	23.4	66.6	10 (Al_2O_3)	2.41
G	20.8	59.2	20 (Al_2O_3)	2.52
H	18.2	51.8	30 (Al_2O_3)	2.63
I	15.6	44.4	40 (Al_2O_3)	2.74

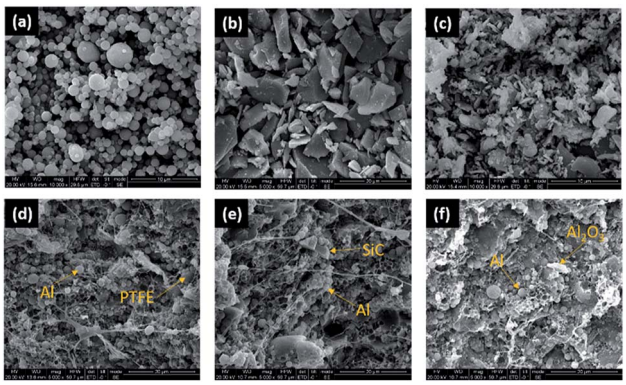

Fig. 1 Microstructures of the composites: (a) Al particles; (b) SiC particles; (c) Al_2O_3 particles; (d) type A; (e) type B; (f) type F.

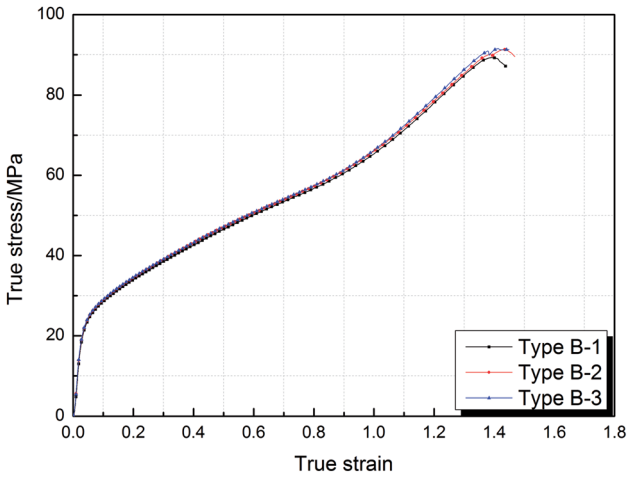

Fig. 2 The true stress–strain curves of the type B sample in triplicate experiments.

Ltd., Shenzhen, Guangdong, China) with a loading capacity of 100 kN, where the load speed was set to 6 mm min^{-1} corresponding to a nominal strain rate of 0.01 s^{-1} at an ambient temperature of 21 °C. Triplicate experiments were conducted for each type of sample to confirm the consistency of the experimental results, and the stress–strain data of the samples were recorded during compression.

A drop-weight instrument was applied to investigate the sensitivity and impact-initiation characteristics of reactive composites. The apparatus has a drop mass of 10 kg, which falls from a variable height in the range of 0 to 156 cm. The samples were placed on an anvil and impacted directly using a free drop hammer. The impact sensitivities of the materials were calculated from the characteristic drop height (H_{50}), at which specimens can have a 50% possibility to react.

The thermal behaviors of the Al/Al_2O_3/PTFE composites were studied using a TG/DSC simultaneous thermal analyzer. Samples with an average mass of 2.0 mg were loaded into the crucible and argon was used as the insured gas at a flow rate of 30 mL min^{-1} to prevent air from participating in the reaction. The device was programmed to heat the samples at a rate of 5 °C min^{-1}, covering the temperature range of 25–1000 °C.

3 Results and discussion

3.1 Mechanical response under quasi-static compression

Taking the experimental results of the type B sample as an example, the stress–strain curves of the type B sample in triplicate experiments presented excellent consistency, as shown in Fig. 2, which indicates that the mechanical data are reliable and reproducible.

Fig. 3 shows the true stress–strain curves of Al/SiC/PTFE and Al/Al_2O_3/PTFE samples under quasi-static compression. The results presented are the average of three samples under identical conditions. It can be observed that all types of samples went through elastic and plastic deformation during compression. Strain hardening phenomenon occurred after the samples reached yield strength. The addition of SiC and Al_2O_3 had a significant influence on the stress–strain curves, and the effect was primarily reflected in the strain hardening stage.

The mechanical property parameters of all types of samples under quasi-static compression calculated based on the stress–strain data are listed in Table 2. The yield strengths and compressive strengths of the Al/SiC/PTFE and Al/Al_2O_3/PTFE samples are compared in Fig. 3. As can be seen, with an increase

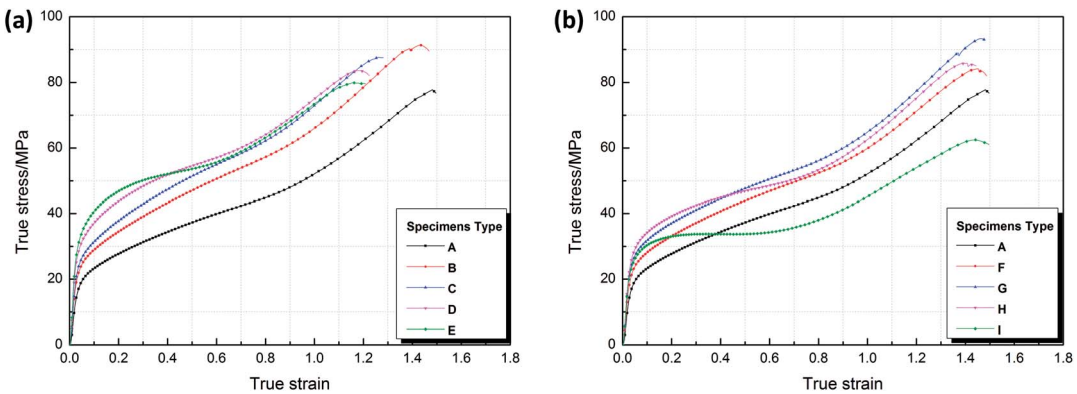

Fig. 3 The true stress–strain curves of samples under quasi-static compression.

Table 2 Mechanical properties of the experimental samples under quasi-static compression

Type	Yield strength/MPa	Elastic modulus/MPa	Hardening modulus/MPa	Compressive strength/MPa	Failure Strain
A	20.49	342.64	29.75	77.81	1.48
B	25.87	401.74	39.28	91.35	1.46
C	28.03	441.25	45.79	87.56	1.26
D	34.84	518.61	34.65	83.54	1.22
E	38.52	539.57	23.98	79.91	1.21
F	25.26	373.48	35.31	84.09	1.48
G	27.68	429.34	35.82	93.33	1.46
H	31.63	468.55	24.59	85.71	1.44
I	28.38	420.53	16.22	64.48	1.49

in the SiC content, the yield strength of the Al/SiC/PTFE samples shows an upward trend, reaching a maximum value of 38.52 MPa for a SiC content of 40 wt%. The yield strengths and compressive strengths of the Al/Al_2O_3/PTFE samples first increase and then subsequently decrease as the Al_2O_3 content increases, which means that an excess of Al_2O_3 destroys the continuity of the PTFE matrix, resulting in the reduction of the strength of the composites. In addition, the yield curves of the Al/SiC/PTFE samples are always above those of the Al/Al_2O_3/PTFE samples, as shown in Fig. 4, indicating that the enhancing effect that SiC has on the material strength is stronger than that of Al_2O_3 in the case of the same ceramic particle content.

Fig. 5 shows the states of the morphologies of the Al/SiC/PTFE and Al/Al_2O_3/PTFE samples after quasi-static compression. It can be seen that the most internally development cracks formed during the failure of the type A specimen, where with an increase in the SiC and Al_2O_3 content, the number of internal cracks decreased correspondingly. Therefore, the addition of SiC and Al_2O_3 effectively inhibit the formation of cracks, resulting in a significant strength increase of the Al/PTFE composites. Fig. 5(f) presents the internal failure morphology of the type A sample cross section. The sample became evidently brittle with typical shear fractures along the 45° planes (the direction of the maximum shear stress in an axially loaded bar).

3.2 Reactive properties under drop-weight tests

The impact sensitivities of all of the types of the Al/SiC/PTFE and Al/Al_2O_3/PTFE samples were calculated from the characteristic drop height (H_{50}), at which the composites have 50% possibility of reacting. The test procedure by which the 50% point is acquired is an application of the so-called "up-and-down technique".[25] In this study, 15 test samples for each type of sample were used. The H_{50} is calculated based on the following formula:

$$H_{50} = \left[A + B\left[\frac{\sum_i N_i}{N} - \frac{1}{2}\right]\right] \quad (1)$$

where A is the lowest height in the experiment, B is the increase in the height, i is the order of the change of height starting from 0, N_i is the number of reaction events under a certain height corresponding to i, and N is the total number of reaction events in all experiments.

The experimental data of the type A, B, C and D samples were recorded according to the "up-and-down technique" and the results are presented in Fig. 6. From eqn (1), the H_{50} values of all of the types of samples were calculated. Fig. 7 depicts the curves of the H_{50} values *vs.* the ceramic particle fractions of the Al/SiC/PTFE and Al/Al_2O_3/PTFE samples. The data show that the sample without ceramic particles has the lowest H_{50} and is the

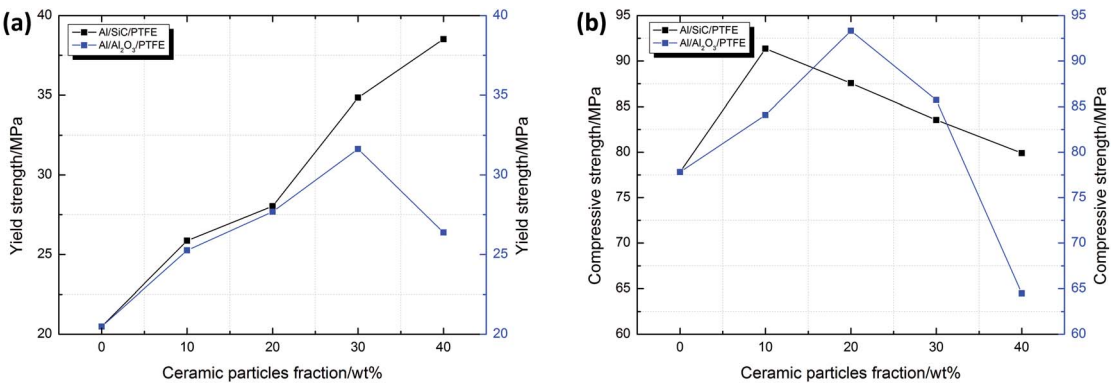

Fig. 4 Comparison of the mechanical properties of the Al/SiC/PTFE and Al/Al_2O_3/PTFE samples.

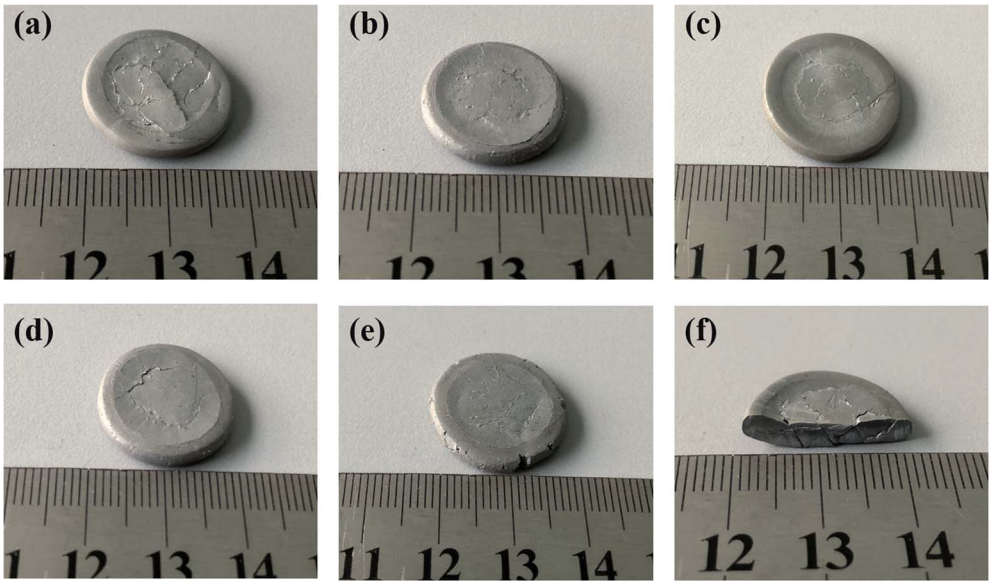

Fig. 5 The states of the morphologies of the Al/SiC/PTFE and Al/Al_2O_3/PTFE samples after quasi-static compression: (a) type A; (b) type B; (c) type D; (d) type F; (e) type H; (f) internal failure morphology of type A.

most sensitive. The H_{50} increased monotonously with an increase in the ceramic particle content, implying that adding ceramic particles to Al/PTFE contributes towards reducing the sensitivity of the reactive composites, but that the degree of influence is different. The effect of Al_2O_3 on the reduction of Al/PTFE sensitivity was weaker than that of SiC. According to the mechanism of hot-spot formation at the crack tip of Al/PTFE proposed by Feng[26] *et al.*, with the addition of ceramic particles, the content of Al/PTFE involved in the reaction decreased, and the hot-spot area formed during the drop impact process was reduced, leading to a diminishing of the composite sensitivity. The difference between SiC and Al_2O_3 in reducing the sensitivity of the composites can be mainly attributed to the addition of SiC, which improves the thermal conductivity of the system, while Al_2O_3 changes the reaction pathway. Besides this, all types of samples reacted under drop hammer impact.

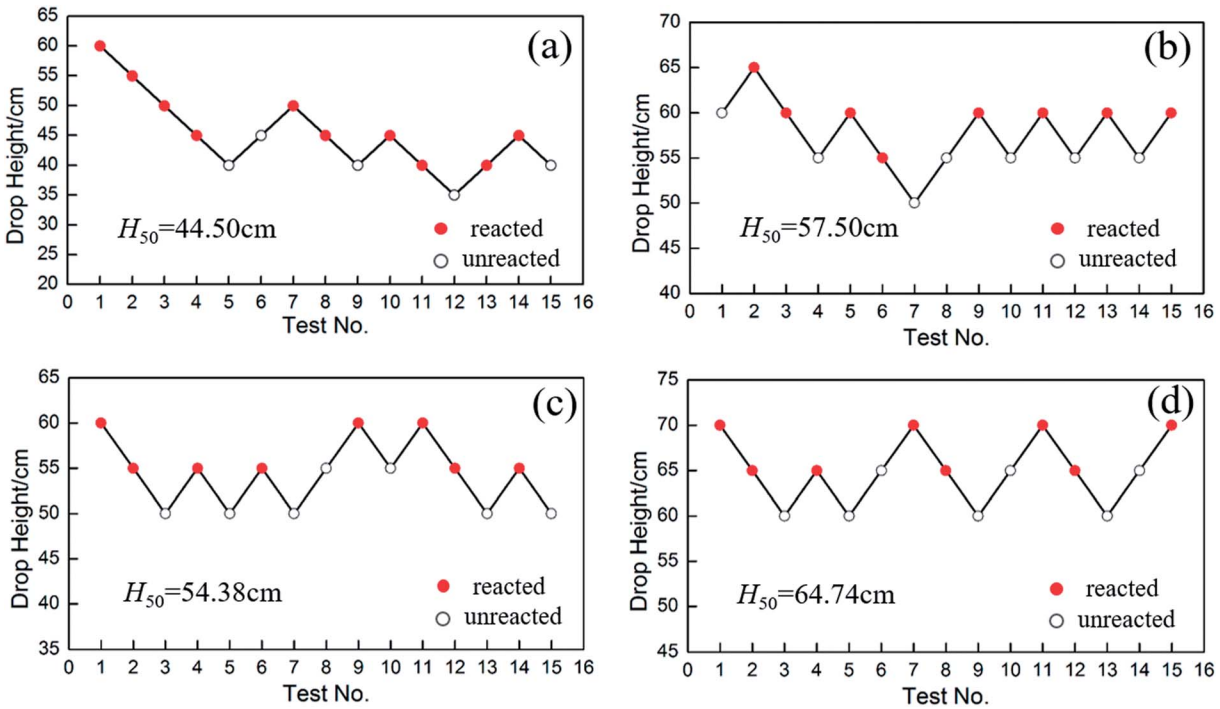

Fig. 6 The drop-weight test data points of selected samples: (a) type A; (b) type B; (c) type C; (d) type D.

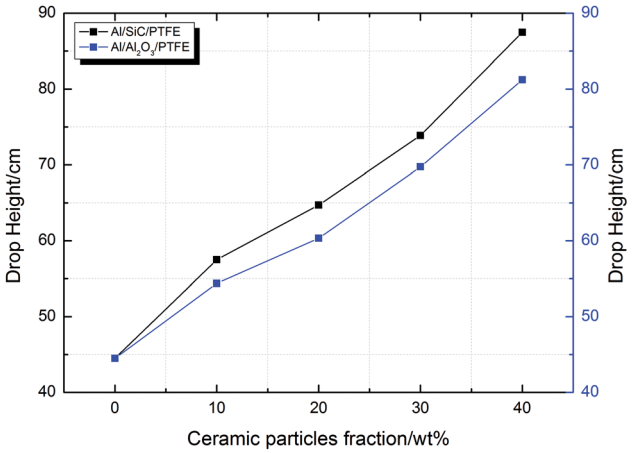

Fig. 7 The H_{50} values of the Al/SiC/PTFE and Al/Al_2O_3/PTFE samples as a function of the ceramic particle fraction.

Combined with the unreacted phenomena under quasi-static compression, it can be concluded that the composites showed different mechanical response and reactive properties under different strain rates, showing that a strain rate effect exists.

3.3 Thermal behavior under TG-DSC tests

Because nanoscale Al and PTFE can undergo pre-ignition reaction (PIR), which is controlled by the fluorination of the Al particle passivation shell (Al_2O_3),[21,22] to gain a better understanding of the thermal reaction process of Al/Al_2O_3/PTFE ternary composites with different particle sizes, the reaction processes of Al/PTFE and Al_2O_3/PTFE were analyzed in advance as references.

3.3.1 Thermal behavior of the Al/PTFE composites. The TG-DSC curves of Al (1 μm)/PTFE and Al (50 nm)/PTFE are depicted in Fig. 8, and the specific parameters of the endothermic and exothermic peaks are summarized in Table 3.

As can be seen from Fig. 8(a), there are three endothermic peaks and one exothermic peak in the DSC curve of the Al (1 μm)/PTFE sample in the process of heating to 800 °C. It can be seen that the endothermic peak A is the melting endothermic peak of the PTFE matrix and the endothermic peak D is the melting endothermic peak of the residual Al powder due to there being no obvious changes in the peaks. The endothermic peak B starts at 508.9 °C, accompanied by the reduction of the sample mass, indicating the formation of gases, which can be considered a product of the decomposition of PTFE. The exothermic peak C starts at 598.1 °C and is thought to be a result of the exothermic reaction between the Al and the decomposition product of PTFE. According to Fig. 8(b), it can be seen that there are two endothermic peaks and two exothermic peaks in the DSC curve of the Al (50 nm)/PTFE sample. Only the properties of peak B changed when compared with the data shown in Fig. 8(a), peak B is endothermic in Fig. 8(a), whereas it is exothermic in Fig. 8(b). The exothermic peak B starts at 485.6 °C and ends at 523.8 °C, and the reaction heat is 4.58 J g^{-1} as a result of the pre-ignition reaction between nanoscale Al and PTFE during heating. The Al_2O_3 layer on the surface of the Al particles reacted with the fluoride ions produced by the condensing of PTFE to form the catalyst AlF_3 in the unstable β-phase.[21] The reaction heat exceeded the heat absorbed by the decomposition of PTFE. Therefore, an exothermic peak B appeared in Fig. 8(b). Besides this, since the specific surface area of the 1 μm Al particles (2.22 m^2 g^{-1}) was significantly smaller than that of the 50 nm Al particles (44.44 m^2 g^{-1}), the Al_2O_3 layer, which participates in the pre-ignition reaction, was correspondingly reduced, and the pre-ignition reaction energy was smaller than the PTFE decomposition absorption energy, leading to the appearance of the endothermic peak B, as shown in Fig. 8(a). In addition, as listed in Table 3, the reaction heat of Al (50 nm)/PTFE was as high as 146.42 J g^{-1}, while that of Al (1 μm)/PTFE was only 0.93 J g^{-1}, which demonstrates that the reaction between the nanoscale Al particles and PTFE was more intense than that of microscale Al particles. Levitas *et al.*[27–29] believed that this was attributed to the unique melt-dispersion mechanism (MDM) of nanoscale Al particles.

3.3.2 Thermal behavior of the Al_2O_3/PTFE composites. Fig. 9 shows the TG-DSC curves of Al_2O_3 (1 μm)/PTFE and Al_2O_3 (30 nm)/PTFE. It can be seen from Fig. 9(a) that there are only two endothermic peaks corresponding to the melting and thermal decomposition of PTFE. No exothermic reaction

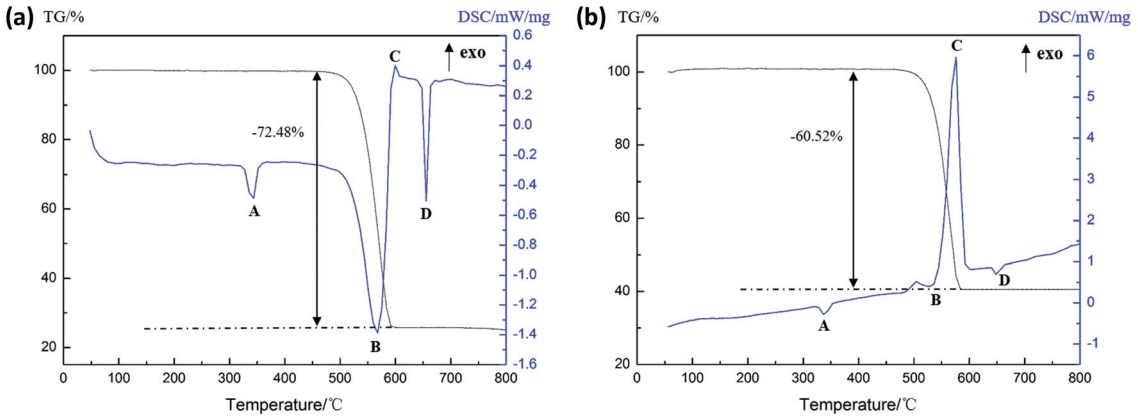

Fig. 8 The TG-DSC curves of (a) Al (1 μm)/PTFE and (b) Al (50 nm)/PTFE.

Table 3 Endothermic and exothermic peak parameters of Al/PTFE composites with different Al particle sizes

Al particle size	No.	Onset temperature/°C	Peak temperature/°C	End temperature/°C	Heat release/J g^{-1}
1 μm	Endo-peak-A	321.9	340.8	354.8	−3.78
	Endo-peak-B	508.9	570.0	589.8	−32.59
	Exo-peak-C	598.1	599.1	606.8	0.93
	Endo-peak-D	648.7	658.8	670.2	−7.42
50 nm	Endo-peak-A	329.3	341.1	352.2	−3.99
	Exo-peak-B	485.6	508.5	523.8	4.58
	Exo-peak-C	536.4	581.3	594.3	146.42
	Endo-peak-D	640.1	649.5	661.2	−3.68

between Al_2O_3 and PTFE can be observed. As Fig. 9(b) indicates, one endothermic peak and two exothermic peaks can be seen in the TG-DSC curve. The exothermic peak B starts at 433.8 °C and corresponds to the reaction between nanoscale Al_2O_3 and PTFE. After the end of the first exothermic reaction, the initial product of the reaction between Al_2O_3 and PTFE was unstable β-phase AlF_3. The exothermic peak associated with the AlF_3 transition from the β to the α phase has been documented to occur at roughly 550 °C.[30–32] Therefore, the exothermic peak C in Fig. 9(b) was formed by the phase transformation of AlF_3.

Pantoya *et al.*[33] studied the influence of alumina passivation on nano-Al/PTFE reactions and the DSC curves as a function of temperature for Al_2O_3/PTFE mixtures with Al_2O_3 according to particle size were measured and the results are shown in Fig. 10. Combined with the phenomenon that the larger the Al_2O_3 particle size, the smaller the area of the exothermic peak, it can be inferred that only nanoscale Al_2O_3 reacts with PTFE, and that the reaction heat decreases with an increase in the Al_2O_3 particle size.

3.3.3 Thermal behavior of the Al/Al_2O_3/PTFE ternary composites. The TG-DSC curves of the three types of Al/Al_2O_3/PTFE samples are shown in Fig. 11. It can be seen that the melting endothermic peaks A of PTFE, the reaction exothermic peaks C between Al and PTFE and the melting endothermic peaks D of residual Al powder existed in all three DSC curves. The differences among the three curves are as follows: for Al (50 nm)/Al_2O_3 (30 nm)/PTFE samples, because Al and Al_2O_3 are nanoscale, the Al_2O_3 shell on the Al surface and the Al_2O_3 of the sample itself can react with PTFE, and as a result there was an obvious pre-ignition reaction phenomenon. The reaction heat outstripped the heat absorbed by the decomposition of the PTFE. Consequently, the exothermic peak B appeared in the DSC curve of Fig. 11(a). For Al (1 μm)/Al_2O_3 (30 nm)/PTFE sample, since Al particles are micron-scale, the Al_2O_3 shell on the surface cannot pre-ignite with PTFE, only nano-Al_2O_3 is able to react with PTFE, but the reaction heat is slightly lower than that absorbed by PTFE decomposition, resulting in the DSC curve taking a downward trend at around 500 °C, corresponding to the endothermic peak B in Fig. 11(b). For Al (1 μm)/Al_2O_3 (1 μm)/PTFE sample, because Al and Al_2O_3 are micron-scale, both the Al_2O_3 shell on the Al surface and the Al_2O_3 of the sample itself cannot react with PTFE, Al_2O_3 only acts as an additive and does not participate in the reaction. In addition, it can be seen from Fig. 11(b) that the reaction heat of the exothermic peak C of the (1 μm)/Al_2O_3 (30 nm)/PTFE sample is 7.86 J g^{-1}. When compared with Fig. 8(a), the reaction heat of the exothermic peak C of the Al (1 μm)/PTFE sample is only 0.93 J g^{-1}, which indicates that adding nanoscale Al_2O_3 to Al-PTFE increases the reaction energy and make the composites react more vigorously. The feasibility of increasing the reaction heat and energy density of the Al/PTFE composites by means of adding Al_2O_3 was proven.

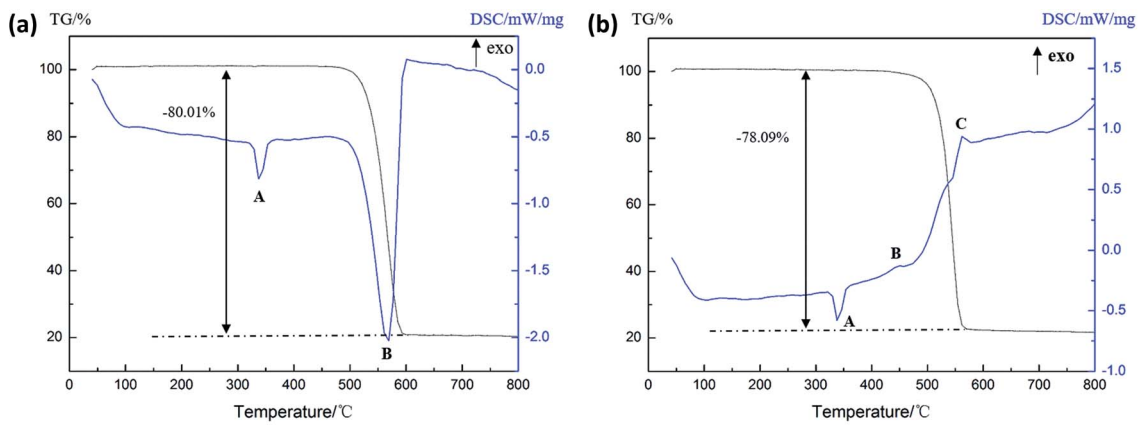

Fig. 9 The TG-DSC curves of (a) Al_2O_3 (1 μm)/PTFE and (b) Al_2O_3 (30 nm)/PTFE.

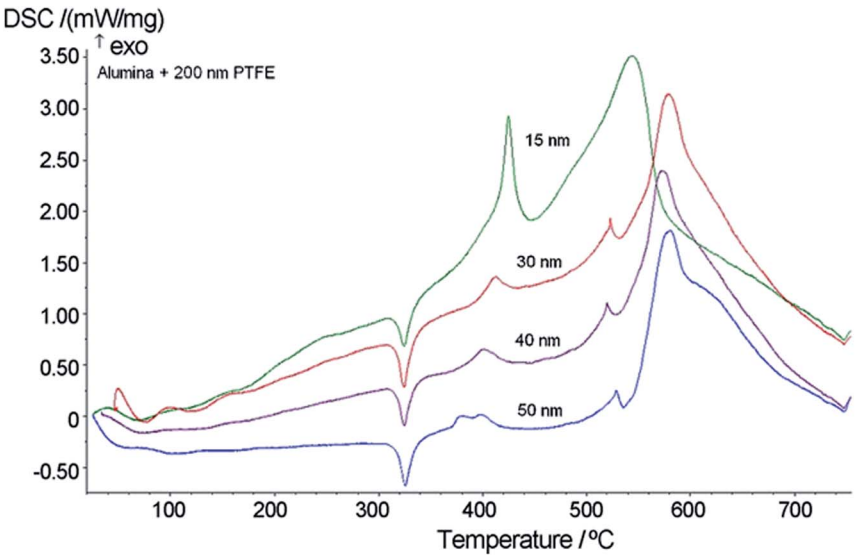

Fig. 10 DSC curves of Al_2O_3/PTFE reactions as a function of Al_2O_3 particle size.

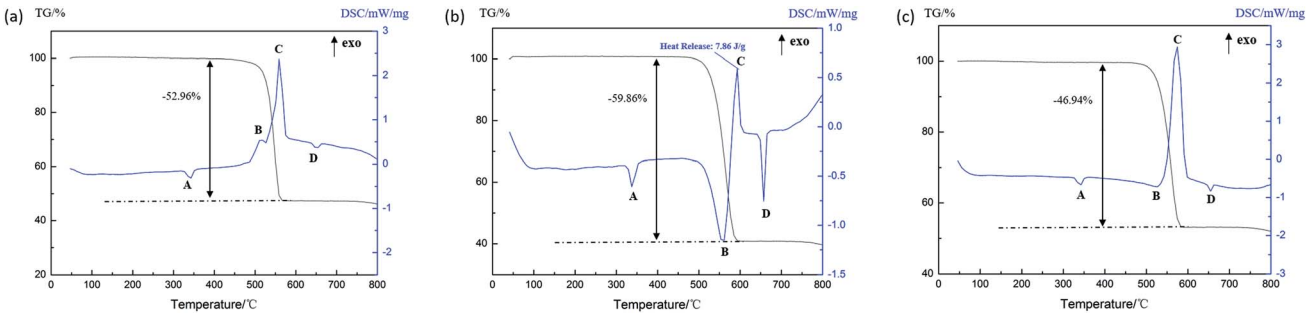

Fig. 11 The TG-DSC curves of the three types of Al/Al_2O_3/PTFE samples. (a) Al (50 nm)/Al_2O_3 (30 nm)/PTFE, (b) Al (1 μm)/Al_2O_3 (30 nm)/PTFE, and (c) Al (1 μm)/Al_2O_3 (1 μm)/PTFE.

4 Conclusions

In this paper, the mechanical response and reactive properties of Al/SiC/PTFE and Al/Al_2O_3/PTFE samples with different contents were studied *via* quasi-static compression and drop-weight tests. The thermal behavior of Al/Al_2O_3/PTFE samples with different particle sizes was ascertained from TG-DSC tests. Conclusions can be drawn as follows:

(1) In quasi-static compression tests, because SiC and Al_2O_3 can effectively inhibit the formation of cracks during compression, the addition of SiC and Al_2O_3 can significantly enhance the strength of Al/PTFE. The enhancing effect of SiC on the composite strength was stronger than that of Al_2O_3.

(2) In drop-weight tests, adding ceramic particles to Al/PTFE contributes towards reducing the sensitivity of the reactive composites, and the reducing effect of Al_2O_3 on the Al/PTFE sensitivity was weaker than that of SiC.

(3) Nanoscale Al_2O_3 reacts with PTFE to form AlF_3, and the reaction heat decreased dramatically with an increase in the Al_2O_3 particle size. The addition of nanoscale Al_2O_3 improved the reaction heat and energy density of the composites.

Conflicts of interest

The authors declare that there is no conflict of interest regarding the publication of this paper.

Acknowledgements

Financial support from the National Natural Science Foundation of China (General Program. Grant No. 51673213) and the National Science Fund for Distinguished Young Scholars (Grant No. 51803235) are gratefully acknowledged.

Notes and references

1 H. Wang, Y. Zheng, Q. Yu, *et al.*, Impact-induced initiation and energy release behavior of reactive materials, *J. Appl. Phys.*, 2011, **110**, 074904.

2 D. B. Nielson, R. M. Truitt and B. N. Ashcroft, Reactive material enhanced projectiles and related methods, *US Pat.*, 7603951, 2009.

3 N. Thadhani, Shock-induced and shock-assisted solid-state chemical reactions in powder mixtures, *J. Appl. Phys.*, 1994, **76**, 2129.
4 W. He, P. J. Liu, G. Q. He, *et al.*, Highly Reactive Metastable Intermixed Composites (MICs): Preparation and Characterization, *Adv. Mater.*, 2018, **30**, 1706293.
5 X. F. Zhang and X. N. Zhao, Review on Multifunctional Energetic Structural Materials, *Chin. J. Energ. Mater.*, 2009, **17**, 731.
6 X. F. Zhang, A. S. Shi, L. Qiao, *et al.*, Experimental study on impact-initiated characters of multifunctional energetic structural materials, *J. Appl. Phys.*, 2013, **113**, 083508.
7 R. J. Lee, W. Mock and J. R. Carney, *et al.*, Reactive Materials Studies, *AIP Conference Proceedings*, 2006.
8 H. A. Miller, B. S. Kusel, S. T. Danielson, *et al.*, Metastable nanostructured metallized fluoropolymer composites for energetics, *J. Mater. Chem. A*, 2013, **24**, 7050.
9 A. Y. Dolgoborodov, M. N. Makhov, I. V. Kolbanev, *et al.*, Detonation in an aluminum–Teflon mixture, *J. Exp. Theor. Phys. Lett.*, 2005, **7**, 311.
10 N. M. Mcgregor and G. T. Sutherland, Plate Impact Experiments on a Porous Teflon–Aluminum Mixture, *AIP Conf. Proc.*, 2004, **706**, 1001.
11 C. Ge, Y. X. Dong and W. Maimaitituersun, Microscale simulation on mechanical properties of Al/PTFE composite based on real microstructures, *Materials*, 2016, **9**, 590.
12 H. F. Wang, H. G. Guo, B. Q. Geng, *et al.*, Application of PTFE/Al Reactive Materials for Double-Layered Liner Shaped Charge, *Materials*, 2019, **12**, 2768.
13 B. Feng, X. Fang, Y. C. Li, *et al.*, An initiation phenomenon of Al-PTFE under quasi-static compression, *Chem. Phys. Lett.*, 2015, **637**, 38.
14 B. Feng, Y. C. Li, S. Z. Wu, *et al.*, A crack-induced initiation mechanism of Al-PTFE under quasi-static compression and the investigation of influencing factors, *Mater. Des.*, 2016, **108**, 411.
15 H. X. Wang, X. Fang, B. Feng, *et al.*, Influence of Temperature on the Mechanical Properties and Reactive Behavior of Al-PTFE under Quasi-Static Compression, *Polymers*, 2018, **10**, 56.
16 J. Y. Lyu, S. W. Chen, W. He, *et al.*, Fabrication of High-Performance Graphene Oxide doped PVDF/CuO/Al Nanocomposites via Electrospinning, *Chem. Eng. J.*, 2019, **368**, 129–137.
17 F. Y. Xu, S. B. Liu, Y. F. Zheng, *et al.*, Quasi-Static Compression Properties and Failure of PTFE/Al/W Reactive Materials, *Adv. Eng. Mater.*, 2017, **19**, 1600350.
18 W. He, P. J. Liu, F. Y. Gong, *et al.*, Tuning the Reactivity of Metastable Intermixed Composite *n*-Al/PTFE by Polydopamine Interfacial Control, *ACS Appl. Mater. Interfaces*, 2018, **10**, 32849.
19 L. Wang, J. X. Liu, S. K. Li, *et al.*, Investigation on reaction energy, mechanical behavior and impact insensitivity of W–PTFE–Al composites with different W percentage, *Mater. Des.*, 2016, **92**, 397.
20 J. Cai, V. F. Nesterenko, K. S. Vecchio, *et al.*, The influence of metallic particle size on the mechanical properties of polytetrafluroethylene-Al–W powder composites, *Appl. Phys. Lett.*, 2008, **92**, 031903.
21 E. Herbold, V. Nesterenko, D. Benson, *et al.*, Particle size effect on strength, failure, and shock behavior in Polytetrafluoroethylene-Al-W granular composite materials, *J. Appl. Phys.*, 2008, **104**, 103903.
22 D. T. Osborne and M. L. Pantoya, Effect of Al Particle Size on the Thermal Degradation of Al/Teflon Mixtures, *Combust. Sci. Technol.*, 2007, **8**, 1467.
23 D. T. Osborne, The effects of fuel particle size on the reaction of Al/Teflon mixtures, PhD thesis, Texas Tech University, Lubbock, TX, USA, 2006.
24 D. B. Nielson, R. L. Tanner and G. K. Lund *US Pat.*, 0116576 A1, Alliant Techsystems Inc. assignee, 2004.
25 W. R. Blackstone, B. Baber and P. M. Ku, New Test Techniques for Evaluating the Compatibility of Materials with Liquid Oxygen under Impact, *ASLE Trans.*, 1968, **11**, 216.
26 B. Feng, Y. C. Li, H. Hao, *et al.*, A Mechanism of Hot-spots Formation at the Crack Tip of Al-PTFE under Quasi-static Compression, *Propellants, Explos., Pyrotech.*, 2017, **42**, 1.
27 V. I. Levitas, M. L. Pantoya and S. Dean, Melt dispersion mechanism for fast reaction of aluminum nano- and micron-scale particles: flame propagation and SEM studies, *Combust. Flame*, 2014, **161**, 1668.
28 K. W. Watson, M. L. Pantoya and V. I. Levitas, Fast reactions with nano- and micrometer aluminum: a study on oxidation versus fluorination, *Combust. Flame*, 2008, **155**, 619.
29 V. I. Levitas, Mechanochemical mechanism for reaction of aluminium nano- and micrometre-scale particles, *Philos. Trans. R. Soc., A*, 2013, **371**, 20120215.
30 H. J. Reitsma and C. Boelhouwer, The catalytic activity of α-AlF_3/Al_2O_3 and β-AlF_3/Al_2O_3, *J. Catal.*, 1974, **33**, 39.
31 A. Moerkerken, B. Behr, M. A. Noordeloos-Maas, *et al.*, The catalytic activity of α- and β-aluminum fluoride, *J. Catal.*, 1972, **24**, 177.
32 Z. Sarbak, Effect of Fluoride and Sodium Ions on Structural and Thermal Properties of γ-Al_2O_3, *Cryst. Res. Technol.*, 1997, **32**, 491.
33 M. L. Pantoya and S. W. Dean, The influence of alumina passivation on nano-Al/Teflon reactions, *Thermochim. Acta*, 2009, **493**, 109.